Heterogeneous Heck Catalysis with Palladium-Grafted Molecular Sieves

Christian P. Mehnert, David W. Weaver, and Jackie Y. Ying*

Contribution from the Department of Chemical Engineering, Massachusetts Institute of Technology, Cambridge, Massachusetts 02139

Received May 20, 1997. Revised Manuscript Received September 30, 1998

Abstract: The synthesis and characterization of palladium-grafted mesoporous MCM-41 material, designated Pd-TMS11, are described. The material is investigated for carbon−carbon coupling reactions (Heck catalysis) with activated and nonactivated aryl substrates. For the preparation of the new catalyst, a volatile organometallic precursor is reacted in the gas phase with the surface of the porous framework, generating a highly dispersed metal deposition. The ultrahigh surface area, the large pore opening, and the highly dispersed catalyst species in Pd-TMS11 material create one of the most active heterogeneous catalysts for Heck reactions.

Introduction

Recently discovered hexagonally packed mesoporous molecular sieves[1] (designated MCM-41) are of great interest to catalysis because their large and uniform pore sizes (20−100 Å) allow sterically hindered molecules facile diffusion to their internal active sites. These nanostructured materials have a well-defined cylindrical pore structure and ultrahigh surface areas of up to 1200 m^2/g, which make them excellent supports for a new generation of heterogeneous catalysts.[2] This research focuses on the synthesis and application of modified mesoporous materials[3,4] that have an active species attached to the framework via host−guest interactions, creating discrete and uniform sites on the inner walls of the porous systems. Due to their large pore sizes (>20 Å), these molecular sieves are of particular interest for catalysis involving bulky substrates, which have been a challenge for zeolitic materials due to their pore opening restrictions (4−12 Å). We have focused our attention on carbon−carbon coupling reactions (Heck catalysis)[5] whereby palladium is used for the olefination of aryl halides with vinyl substrates, forming bulky coupling products. Heck catalysis is one of the most versatile tools in modern synthetic chemistry and has great potential for future industrial applications. Although recent advances in homogeneous[6] and heterogeneous[7] Heck catalysis have attracted considerable attention, these catalysts currently suffer from several drawbacks, such as low turnover numbers (TON) and limited lifetime.[8]

* To whom correspondence should be addressed.

(1) (a) Kresge, C. T.; Leonowicz, M. E.; Roth, W. J.; Vartuli, J. C.; Beck, J. S. *Nature* **1992**, *359*, 710−712. (b) Beck, J. S.; Vartuli, J. C.; Roth, W. J.; Leonowicz, M. E.; Kresge, C. T.; Schmitt, K. D.; Chu, C. T-W.; Olson, D. H.; Sheppard, E. W.; McCullen, S. B.; Higgens, J. B.; Schlenker, J. L. *J. Am. Chem. Soc.* **1992**, *114*, 10834−10843.

(2) Reviews: (a) Ying, J. Y.; Mehnert, C. P.; Wong, M. S. *Angew. Chem.* **1998**, in press. (b) Sayari, A. *Chem. Mater.* **1996**, *8*, 1840−1852. (c) Behrens, P. *Adv. Mater.* **1993**, *5*, 127−132.

(3) Mehnert, C. P.; Ying, J. Y. *Chem. Commun.* **1997**, 2215−2216.

(4) (a) Ryoo, R.; Jun, S.; Kim, J. M.; Kim, M. J. *Chem. Commun.* **1997**, 2225−2226. (b) Yonemitsu, M.; Tanaka, Y.; Iwamoto, M. *Chem. Mater.* **1997**, *9*, 2679−2681. (c) Maschmeyer, T.; Oldroyd, R. D.; Sankar, R. D.; Thomas, J. M.; Shannon, I. J.; Klepetko, J. A.; Masters, A. F.; Beatie, J. K.; Catlow, C. R. A. *Angew. Chem., Int. Ed. Engl.* **1997**, *109*, 11713−1716. (d) Diaz, J. F.; Balkus, K. J., Jr.; Bedioui, F.; Kurshev, V.; Kevan, L. *Chem. Mater.* **1997**, *9*, 61−67. (e) Liu, C.-J.; Li, S. G.; Pang, W.-Q.; Che, C.-M. *Chem. Commun.* **1997**, 65−66. (f) Maschmeyer, T.; Rey, F.; Sankar, G.; Thomas, J. M. *Nature* **1995**, *378*, 159−162. (g) Morey, M.; Davidson, A.; Eckert, H.; Stucky, G. *Chem. Mater.* **1996**, *8*, 486−492. (h) Rao, Y. V. S.; De Vos, D. E.; Bein, T.; Jacobs, P. A. *Chem. Commun.* **1997**, 355−356. (i) Sutra, P.; Brunel, D. *Chem. Commun.* **1996**, 2485−2486. (j) Wu, C.-G.; Bein, T. *Chem. Mater.* **1994**, *6*, 1109−1112. (k) Zhang, W.; Wang, J.; Tanev, P. T.; Pinnavaia, T. J. *Chem. Commun.* **1996**, 979−980. (l) Abdel-Fattah, T. M.; Pinnavaia, T. J. *Chem. Commun.* **1996**, 665−666. (m) Abe, T.; Tachibana, Y.; Uematsu, T.; Iwamoto, M. *Chem. Commun.* **1995**, 1617−1618. (n) Butterworth, A. J.; Clark, J. H.; Walton, P. H.; Barlow, S. J. *Chem. Commun.* **1996**, 1857−1858. (o) Zhang, Z.; Suo, J.; Zhang, X.; Li, S. *Chem. Commun.* **1998**, 241−242. (p) Van Rhijin, W. M.; De Vos, D. E.; Sels, B. F.; Bossaert, W. D.; Jacobs, P. A. *Chem. Commun.* **1998**, 317−318. (q) Rao, Y. V. S.; De Vos, D. E.; Jacobs, P. A. *Angew. Chem., Int. Ed. Engl.* **1997**, *36*, 2661−2663. (r) Fowler, C. E.; Burkett, S. L.; Mann, S. *Chem. Commun.* **1997**, 1769−1770. (s) Macquarrie, D. J.; Jackson, D. B. *Chem. Commun.* **1997**, 1781−1782.

(5) Reviews: (a) Herrmann, W. A. In *Applied Homogeneous Catalysis with Organometallic Compounds*; Cornils, B., Herrmann, W. A., Eds.; VCH: Weinheim, Germany, 1996; Vol. 2, pp 712−732. (b) Cabri, W.; Candiani, I. *Acc. Chem. Res.* **1995**, *28*, 2−7. (c) Daves, G. D., Jr.; Hallberg, A. *Chem. Rev.* **1989**, *89*, 1433−1445. (d) de Meijer, A.; Meyer, F. E. *Angew. Chem., Int. Ed. Engl.* **1994**, *33*, 2379−2411. (e) Grushin, V. V.; Alper, H. *Chem. Rev.* **1994**, *94*, 1047−1062.

(6) (a) Beller, M.; Fischer, H.; Herrmann, W. A.; Öfele, K.; Brossmer, C. *Angew. Chem., Int. Ed. Engl.* **1995**, *34*, 1848−1849. (b) Beller, M.; Riermeier, T. H. *Tetrahedron Lett.* **1996**, *37*, 6535−6538. (c) Beller, M.; Riermeier, T. H.; Haber, S.; Kleiner, H.-J.; Herrmann, W. A. *Chem. Ber.* **1996**, *129*, 1259−1264. (d) Ben-David, Y.; Portnoy, M.; Milstein, D. *Organometallics* **1992**, *11*, 1995−1996. (e) Herrmann, W. A.; Elison, M.; Fischer, J.; Köcher, C.; Artus, G. R. J. *Angew. Chem., Int. Ed. Engl.* **1995**, *34*, 2371−2374. (f) Jeffery, T. *Tetrahedron Lett.* **1994**, *35*, 3051−3054. (g) Loiseleur, O.; Meier, P.; Pfaltz, A. *Angew. Chem., Int. Ed. Engl.* **1996**, *35*, 200−202. (h) Portnoy, M.; Ben-David, Y.; Milstein, D. *Organometallics* **1994**, *13*, 3465−3479. (i) Herrmann, W. A.; Brossmer, C.; Öfele, K.; Reisinger, C.-P.; Priermeier, T.; Beller, M.; Fischer, H. *Angew. Chem., Int. Ed. Engl.* **1995**, *34*, 1844−1848. (j) Herrmann, W. A.; Brossmer, C.; Öfele, K.; Beller, M.; Fischer, H. *Mol. Catal. A* **1995**, *103*, 133−146. (k) Herrmann, W. A.; Brossmer, C.; Reisinger, C.-P.; Riermeier, T. H.; Öfele, K.; Beller, M. *Chem. Eur. J.* **1997**, *3*, 1357−1364. (l) Reetz, M. T.; Lohmer, G.; Schwickardi, R. *Angew. Chem.* **1998**, *110*, 492−495. (m) Reetz, M. T.; Lohmer, G.; Schwickardi, R. *Angew. Chem., Int. Ed. Engl.* **1997**, *36*, 1526−1529. (n) Ohff, M.; Ohff, A.; van der Boom, M. E.; Milstein, D. *J. Am. Chem. Soc.* **1997**, *119*, 11687−11688.

(7) (a) Reetz, M. T.; Lohmer, G. *Chem. Commun.* **1996**, 1921−1922. (b) Augustine, R. L.; O'Leary, S. T. J. *Mol. Catal. A* **1992**, *72*, 229−242. (c) Augustine, R. L.; O'Leary, S. T. J. *Mol. Catal. A* **1995**, *95*, 277−285. (d) Beller, M.; Kühlein, K. *Synlett* **1995**, 441−442. (e) Beller, M.; Fischer, H.; Kühlein, K.; Reisinger, C.-P.; Herrmann, W. A. *J. Organomet. Chem.* **1996**, *520*, 257−259.

(8) (a) Baumeister, P.; Seifert, G.; Steiner, H. (Ciba-Geigy), EP Patent No. A 584 043, **1992**. (b) Beller, M.; Tafesh, A.; Herrmann, W. A. DE Patent No. 19 503 119, **1996**. (c) DeVries, R. A.; Mendoza, A. *Organometallics* **1994**, *13*, 2405−2411.

10.1021/ja971637u CCC: $15.00
Published on Web 11/12/1998

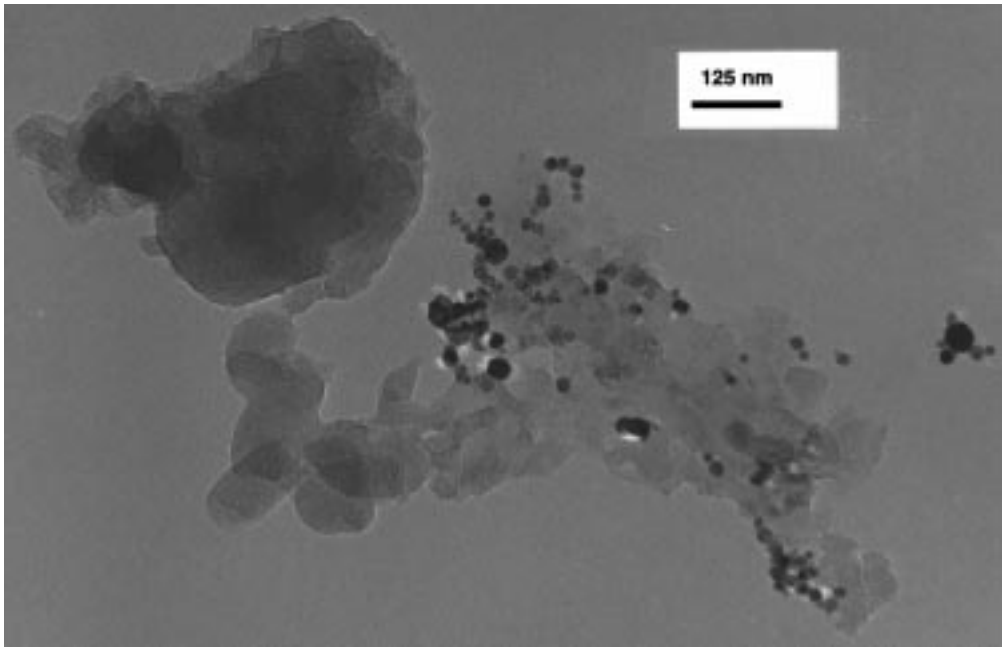

Figure 1. Transmission electron micrograph of palladium-containing Nb-MCM-41 material prepared via impregnation with $PdCl_2$.

Herein we report the synthesis and characterization of palladium-grafted mesoporous materials, designated Pd-TMS11, and their evaluation as heterogeneous catalysts for Heck reactions of activated and nonactivated aryl substrates.

Results and Discussions

In our effort to design a heterogeneous Heck catalyst, we synthesized the mesoporous Pd-TMS11 material, which has highly dispersed palladium and the ability to accommodate sterically demanding substrates. Due to the easy accessibility of its large pores, mesoporous Nb-MCM-41 material was employed as the support framework for the deposition of the catalytically active species. For the preparation of palladium-loaded mesoporous materials, we initially applied the impregnation method. After treating porous Nb-MCM-41 material with an aqueous solution of $PdCl_2$, the resulting material was reduced under a stream of hydrogen, giving a gray palladium-containing powder. The isolated material retained its hexagonally packed porous structure (XRD: (100) 40.4 Å, (110) 22.8 Å, (200) 19.8 Å, (210) 14.9 Å) with a high surface area (948 m^2/g) and a palladium loading of 1.0 wt %. Although the well-defined pore structure of the Nb-MCM-41 material was intact, the palladium dispersion on the surface was only 9%. Investigation of the impregnated material with TEM (Figure 1) and EDAX mapping showed the formation of palladium clusters on the porous support materials, which accounted for the low palladium metal dispersion. In an impregnation experiment with the organometallic complex[9] [Pd(η-C_5H_5)(η^3-C_3H_5)] as the palladium source, a metal dispersion of 17% was established and was the highest value obtained via the impregnation technique. A comparison of metal dispersions for various palladium-containing materials is shown in Table 1. Further impregnation attempts were undertaken to prepare highly dispersed palladium inside the porous framework of Nb-MCM-41, but the majority of the samples showed substantial cluster formation.

Therefore, a different approach was adopted that involved introduction of palladium species from the vapor phase.[10] Palladium-grafted mesoporous material, designated Pd-TMS11, was made by vapor deposition of a volatile palladium complex onto the walls of the porous framework, followed by reduction with H_2. The success of grafting the inside of a porous material with a highly dispersed metal film strongly depends on the properties of the volatile complex and the reaction conditions. To maintain the uniform structure, high surface area, and accessibility of the mesoporous support, it is important to minimize cluster growth inside and outside the molecular sieve. Vapor grafting provides a uniform distribution of volatile complex, and ensures the discrete deposition of metal fragments throughout the porous structure of the support without cluster formation, giving metal-grafted molecular sieves.

Table 1. Palladium-Containing Catalysts Prepared via Impregnation or Vapor Grafting Techniques

Pd-containing material (method, precursor)	Pd (wt %)	metal dispersion (%)	metal surface area (m^2/g Pd)
Pd/SiO_2 (impregnation, $PdCl_2$)	2.0	4	18
Pd/Al_2O_3 (impregnation, $PdCl_2$)[a]	9.1	15	60
Pd/Nb-MCM-41 (impregnation, $PdCl_2$)	1.0	9	40
Pd/Nb-MCM-41 (impregnation, [Pd(η-C_5H_5)(η^3-C_3H_5)])	4.4	17	78
Pd-TMS11[s] (vapor grafting, [Pd(η-C_5H_5)(η^3-C_3H_5)])[b]	1.6	25	110
Pd-TMS11 (vapor grafting, [Pd(η-C_5H_5)(η^3-C_3H_5)])	22.3	32	140

[a] From Sigma-Aldrich. [b] Silanized Nb-MCM-41 material was used as the support.

The Nb-MCM-41 support material was prepared by using a slightly modified procedure from that reported by Mobil researchers. This gave materials with BET surface areas of 950−1050 m^2/g and pore diameters of 24−28 Å. The palladium grafting of the degassed Nb-MCM-41 material was carried out via sublimation of the volatile organometallic complex [Pd(η-C_5H_5)(η^3-C_3H_5)] under reduced pressure through the porous

(9) Shaw, B. L. *J. Chem. Soc.* **1960**, 247.

(10) (a) Zinn, A. A.; Brandt, L.; Kaesz, H. D.; Hicks, R. F. In *Chemical Vapor Deposition of Platinum, Palladium and Nickel*; Kodas, T. T., Hampden-Smith, M. J., Eds.; VCH: Weinheim, Germany, 1994; pp 329−355. (b) Gates, B. C. In *Metal Cluster Catalysts Dispersed on Solid Supports*; Adams, R. D., Cotton, F. A., Eds.; Wiley-VCH: New York, 1998; pp 509−538. (c) Kirillov, V. L.; Zaikovskii, V. I.; Ryndin, Yu. A. *React. Kinet. Catal. Lett.* **1998**, *64*, 169−175.

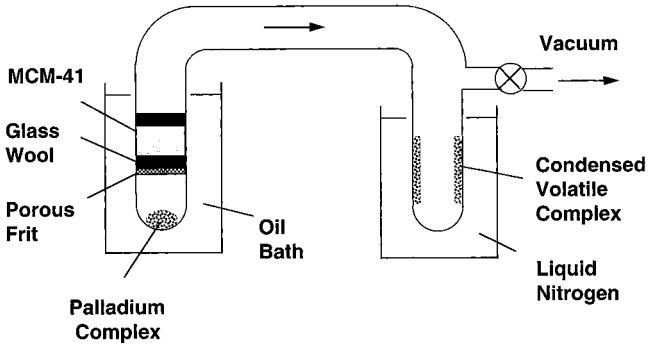

Figure 2. Apparatus for the preparation of vapor-grafted Pd-TMS11.

Scheme 1

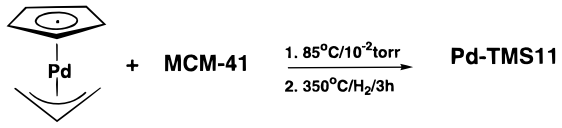

material (Scheme 1). The volatile palladium complex was loaded in a small round-bottom flask and attached to a short-path frit (Figure 2). After the degassed Nb-MCM-41 material was loaded onto the porous frit and secured with a layer of glass wool, a condensation bridge with a cold trap was attached and evacuated to 10^{-2} Torr. The round-bottom flask with palladium precursor and the frit with Nb-MCM-41 were placed in an oil bath that was heated to 85 °C. It is important that the oil bath fully covers the frit with the Nb-MCM-41 material during the vapor grafting process, as otherwise the volatile palladium complex condenses in excess on the porous support. In a successful grafting reaction, the white-colored Nb-MCM-41 material turned uniformly grayish-black, and excess volatile palladium complex could be recovered as red crystals from the cold trap. After the palladium complex had been deposited onto the walls of the porous framework, the material was reduced under a stream of hydrogen at 350 °C for 3 h, yielding an air-stable, black powder. Following the above procedure, materials with typical palladium loadings of 20−25 wt % were obtained. The level of palladium loading depends on the condition used in the Nb-MCM-41 pretreatment, which controls the number of reactive oxygen groups that are available for reaction with the palladium complex. For example, Nb-MCM-41 that had been heated and degassed under reduced pressure (10^{-2} Torr, 600 °C) gave palladium loadings between 20 and 25 wt %, whereas material degassed under milder condition (10^{-2} Torr, 150 °C) led to palladium loadings between 15 and 20 wt %. In both cases, the degassed Nb-MCM-41 was exposed to an excess of volatile palladium precursor. When the amount of the palladium complex was reduced, the resulting sample would not be uniformly grafted with palladium. This was readily noticeable, since the palladium precursor would be consumed by the lower level of the Nb-MCM-41 bed, while the top part of the bed remained untreated.

In an effort to significantly reduce the palladium content of the material while maintaining a uniform Pd distribution, silanized Nb-MCM-41 (Scheme 2) was used as the support material. The fractional capping of the reactive hydroxy groups with an inert silane fragment reduced the susceptibility of the support surface to electrophilic attack, providing a convenient method for synthesizing Pd-grafted materials (designated Pd-TMS11^s) with much lower levels of palladium loading (values as low as 1.6 wt % were obtained). Although the palladium loading was reduced in Pd-TMS11^s, the metal dispersion did not exceed 30% and was in a similar range to that for Pd-TMS11 with loadings of 15−25 wt %.

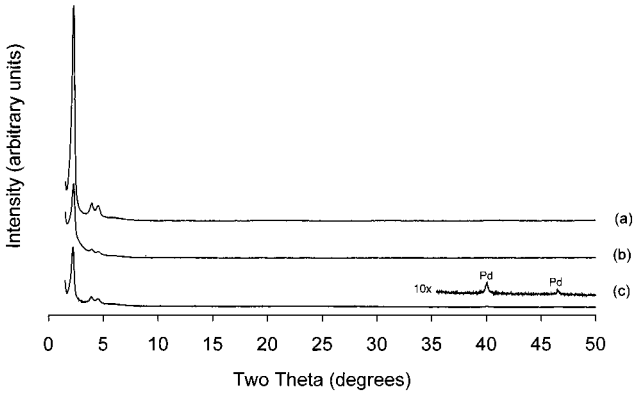

Figure 3. Powder XRD patterns of (a) MCM-41 starting material, (b) Pd-TMS11 catalyst after H_2 reduction, and (c) Pd-TMS11 catalyst recovered after a TON of 3000.

Scheme 2

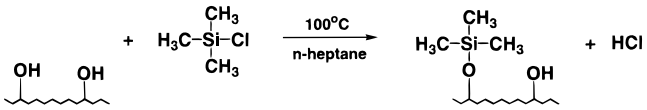

Following the successful synthesis of uniformly grafted Pd-TMS11^s material with a reduced palladium content, we scaled up the vapor grafting technique. To ensure uniform exposure of large amounts of support material to the volatile palladium complex during the vapor grafting process, a fluidized bed reactor was designed and constructed. The silanized Nb-MCM-41 material and the organometallic precursor were loaded under an inert atmosphere, before a stream of argon saturated with the volatile palladium precursor was applied to generate the fluidized bed. After the column was heated to 125 °C for 2 h, the white Nb-MCM-41 material turned grayish-black and an excess of the palladium complex was deposited at the top of the column. The unreacted palladium complex was recycled, and the grafted porous material was reduced under a stream of hydrogen, producing the Pd-TMS11^s catalyst on a multigram scale.

The Pd-TMS11 catalyst retained its hexagonally packed porous structure as shown by the XRD pattern (Figure 3b). Although the diffraction patterns of Pd-TMS11 and the MCM-41 starting material (Figure 3a) have similar peaks, the peak intensity for Pd-TMS11 was lower, possibly due to radiation diffusion caused by the grafted palladium metal. Palladium metal has major diffraction peaks at $2\theta = 40.1°$ (111) and 46.7° (200), which were not found in the XRD pattern of Pd-TMS11 (Pd content: 19.1 wt %), indicating that palladium was highly dispersed in the latter. The BET surface area of a typical Pd-TMS11 sample with a palladium content of 19.1 wt % was 750 m^2/g by N_2 adsorption (Figure 4). The BJH (Brunauer−Joyner−Halenda) pore size distribution of Pd-TMS11 had a narrow peak centered at 26.1 Å, which was, as expected, slightly smaller than that determined for the MCM-41 starting material (27.4 Å) due to the presence of grafted palladium metal in Pd-TMS11. TEM examination indicated the hexagonally packed pore structure of Pd-TMS11 (Figure 5), with no noticeable palladium clusters. In addition, energy dispersive analysis by EDAX on Pd-TMS11 particles indicated that palladium was highly dispersed over the pore surface of the mesoporous support (Figure 6).

Elemental analysis of Pd-TMS11 showed palladium metal contents between 1 and 25 wt %, depending on the pretreatment of the MCM-41 starting material and the amount of volatile complex [Pd(η-C_5H_5)(η^3-C_3H_5)] used in the vapor grafting

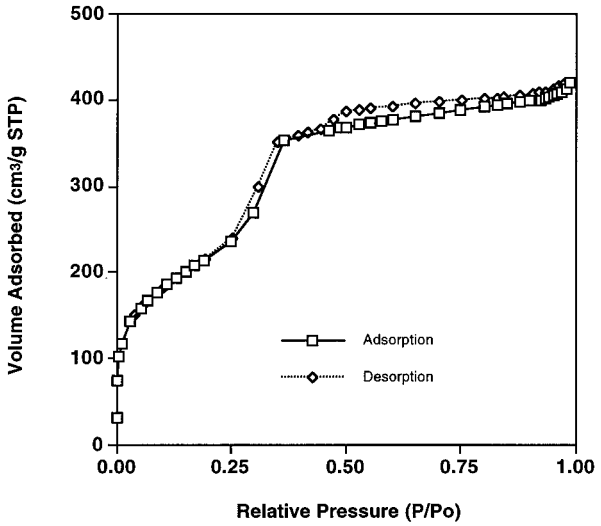

Figure 4. N_2 adsorption−desorption isotherm of Pd-TMS11 with a Pd content of 19.1 wt %.

process (Table 1). CO chemisorption on Pd-TMS11 showed metallic surface areas between 110 and 140 m^2/g (Pd metal), with a metal dispersion as high as 32%. In comparison, materials prepared by using impregnation methods showed dispersions between 4% and 17% and metallic surface areas of 18−78 m^2/g (Pd metal). Although a metal dispersion of 17% was obtained with the complex [Pd(η-C_5H_5)(η^3-C_3H_5)] in solution impregnation, introduction of the same complex via the gas phase generated metal dispersions as high as 32%, clearly demonstrating the advantages of the vapor grafting approach.

The Pd-TMS11 materials catalyzed the Heck carbon−carbon coupling reactions (Scheme 3). The catalytic activity of these materials was investigated with activated and nonactivated aryl halides, with styrene or *n*-butyl acrylate as the vinylic substrate. The reactions were conveniently carried out in batch reactors in air with temperatures between 120 and 170 °C (Table 2). The yields for the activated aryl halides with respect to reaction time and amount of catalyst showed that *n*-butyl acrylate is a more reactive substrate than styrene. Investigation of the kinetics of the reaction of *n*-butyl acrylate with 4-bromoacetophenone (Figure 7) showed a typical initiation period of 5 min required to heat the reaction mixture to the appropriate temperature. Addition of catalyst to a preheated reaction mixture resulted in instantaneous reactions. Full conversion and a yield of 99% were obtained after only 1 h for the reaction of *n*-butyl acrylate and 4-bromoacetophenone with as little as 0.02 mol % catalyst. Reaction between bromobenzene and *n*-butyl acrylate at 170 °C gave a TON of 624, which is higher than that achieved by many of the most active homogeneous Heck catalysts.[6] To ensure that no reactive palladium was dissolved in the reaction mixture, we isolated the catalyst after 20% conversion and monitored the resulting filtrate under identical reaction condition for another 2 h; no further conversion was detected on removal of Pd-TMS11. Addition of elemental mercury to a progressing reaction resulted in the immediate poisoning of the catalyst. Both studies indicated a reaction mechanism based on a heterogeneous catalysis cycle for carbon−carbon bond formation with Pd-TMS11.

For further comparison, we investigated commercially available palladium catalysts (supported on silica, alumina, and carbon), as well as palladium-impregnated Nb-MCM-41. Compared to Pd-TMS11, these systems showed significantly lower reactivity (up to 70% conversion for the activated aryl substrates) with respect to their total TON, which might be attributed to their low palladium dispersion (e.g. metal dispersion was only 4% for palladium on silica), and with the exception of the impregnated Nb-MCM-41 sample, to limited diffusion in the micropores of the support materials. Investigation of nonactivated aryl substrates gave only negligible conversion over the impregnated palladium materials. However, surprisingly high conversions were achieved for the nonactivated aryl substrates with Pd-TMS11 (67% for bromobenzene with *n*-butyl acrylate),

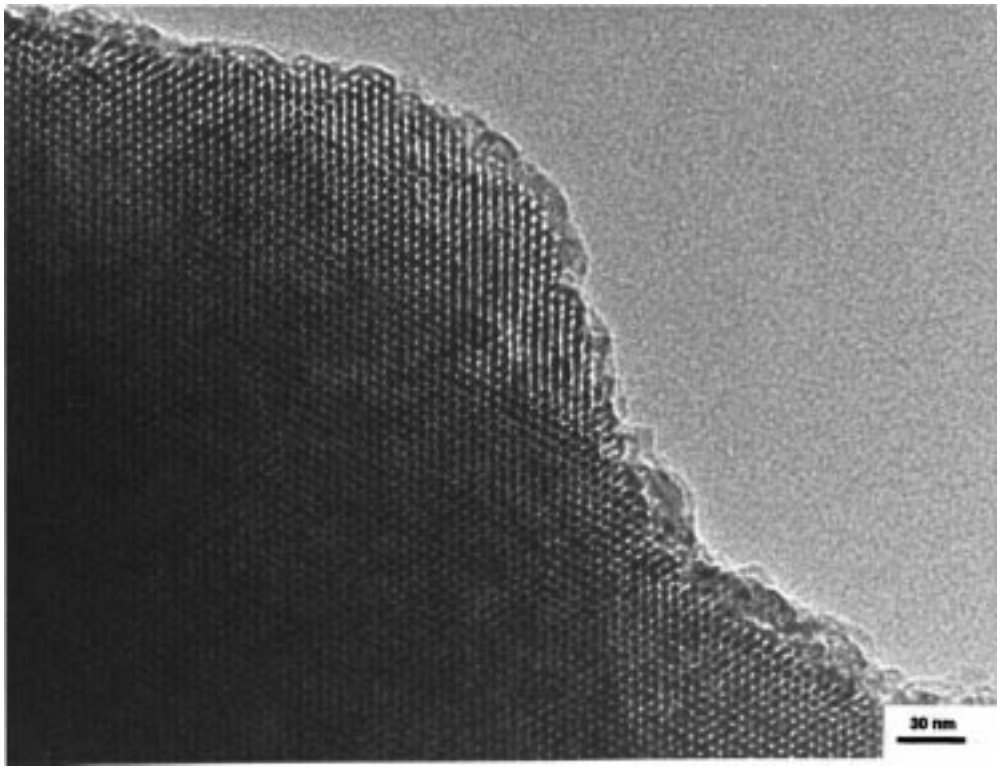

Figure 5. Transmission electron micrograph of vapor-grafted Pd-TMS11.

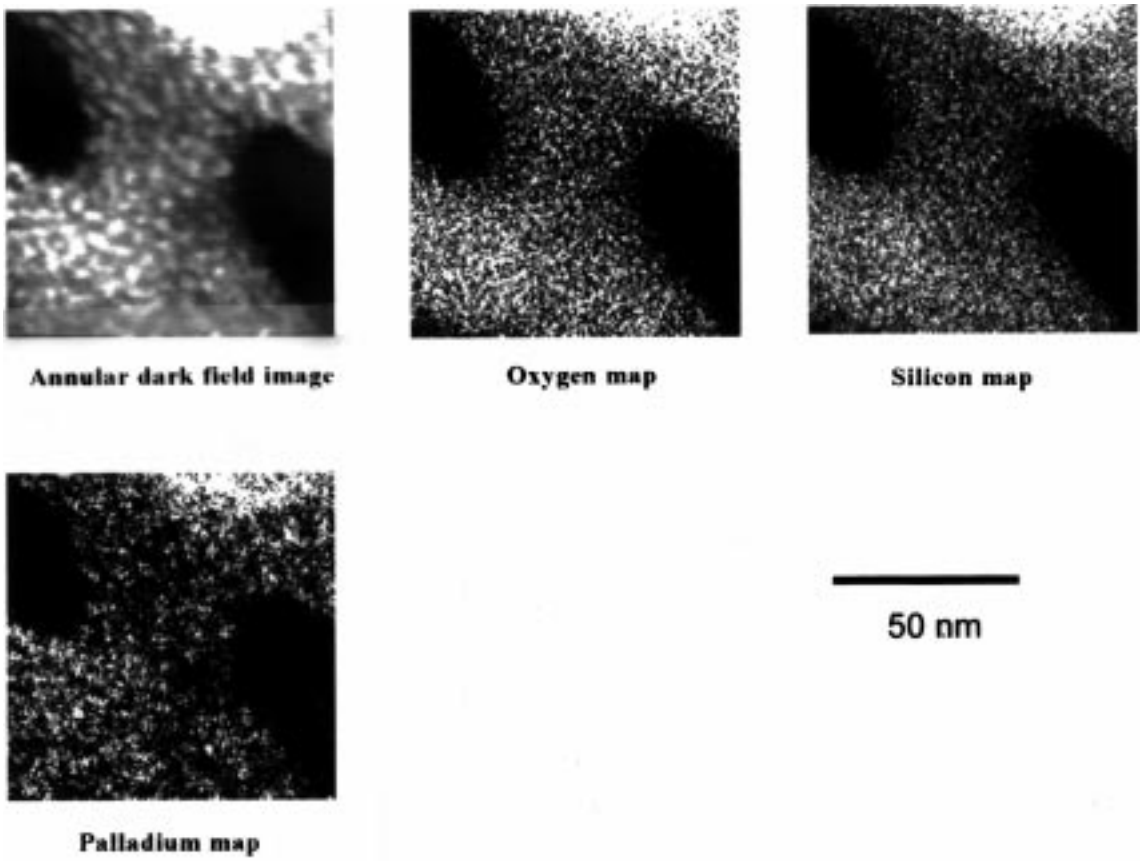

Figure 6. EDAX study of Pd-TMS11. Top row: annular dark field (ADF) image (left), oxygen map (middle), and silicon map (right). Bottom row: palladium map (left).

Table 2. Heck Olefination[a] of Aryl Halides Over Pd-TMS11 Catalysts

vinyl substrate	aryl halide substrate[b]	amount of catalyst (mol %)	*T* (°C)	time	% conversion[c] (% yield)[d]	*E*:*Z*	TON[e]
styrene	C_6H_5Br	0.1	170	48 h	39 (82)	99:1	200
	4-$BrC_6H_4NO_2$	1.0	120	20 min	99 (98)	95:5	50
	4-$BrC_6H_4NO_2$	0.1	120	8 h	98 (99)	96:4	500
	4-$BrC_6H_4C(O)CH_3$	0.1	120	45 min	99 (98)	95:5	1000
n-butyl acrylate	C_6H_5Cl	0.1	170	32 h	16 (40)	99:1	64
	C_6H_5Br	0.1	170	48 h	67 (92)	99:1	624
	4-$BrC_6H_4NO_2$	0.1	120	90 min	100 (99)	99:1	1000
	4-$BrC_6H_4C(O)CH_3$	0.1	120	25 min	100 (99)	99:1	1000
	4-$BrC_6H_4C(O)CH_3$	0.02	120	60 min	100 (99)	99:1	5000

[a] All reactions were carried out in air. [b] 1.1 equiv of base [$N(CH_2CH_3)_3$] with respect to the aryl halide substrate was added to the reaction mixture. [c] Conversion of reactant was determined by gas chromatography. [d] Yield = (mol of coupling product (*E*+*Z*))/(mol of reactant converted). [e] TON = (mol of product)/(mol of catalyst).

although systems with even higher activity are needed for efficient industrial applications.

Advantages of the Pd-TMS11 material were that the catalytic reactions could be conveniently carried out in air, and the separation of this heterogeneous catalyst could be achieved easily by filtration. The recovered Pd-TMS11 catalyst showed some agglomeration of palladium and partial structural damage of the Nb-MCM-41 support material. Detailed studies were carried out on Pd-TMS11 material that had been recovered after three catalysis cycles in the reaction between *n*-butyl acrylate and 1-bromo-4-nitrobenzene, with a total TON of 3000. The XRD pattern (Figure 3c) of the used catalyst showed reduced intensity for the diffraction peaks at low 2θ angles for the porous framework of the support. Between $2\theta = 40°$ and 50°, two XRD peaks for palladium were noted, which indicated metal cluster formation. The widths of these diffraction peaks were too broad to allow a precise crystallite size determination. The BET surface

Scheme 3

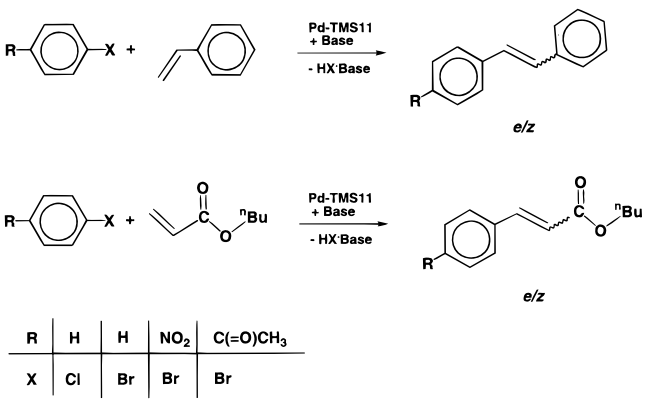

area and average pore diameter of the used catalyst were 780 m^2/g and 27 Å, respectively, compared to 750 m^2/g and 26 Å

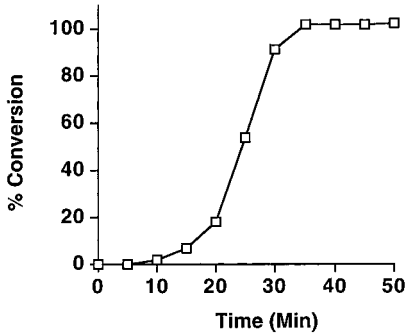

Figure 7. Conversion as a function of time for Heck olefination of 4-bromoacetophenone (as an example for activated aryl substrate) with *n*-butyl acrylate at 120 °C with 0.02 mol % Pd-TMS11 catalyst. For reaction conditions, see Table 2.

before catalysis. Elemental analysis of the used catalyst showed a palladium content reduced by ~5 wt % (for Pd-TMS11 catalysts with 20−25 wt % loading) and an increase in the carbon content to ~4 wt %, indicating loss of palladium and some coking of the catalyst surface. TEM (Figure 8) and EDAX examination showed the formation of some palladium clusters and partial structural damage of the Nb-MCM-41 support in the used catalyst. The palladium clusters had a typical crystallite size of 150 Å and a tendency to agglomerate over time. Although the Pd-TMS11 catalyst suffered from deactivation after long periods of reaction, the palladium metal could be almost fully recovered. The Pd-TMS11 system is an extremely simple and efficient Heck catalyst that rivals the best homogeneous catalysts in use today.

Conclusions

A new heterogeneous catalyst system Pd-TMS11 has been successfully prepared by *vapor grafting*. Mesoporous Nb-MCM-41 was used as the support since its well-defined, large pore opening provided easy access for large substrate molecules. The introduction of palladium from the vapor phase resulted in highly dispersed metal sites on the pore walls of the support material, providing excellent activity for Heck carbon−carbon coupling reactions in air.

Experimental Section

Materials. Sodium silicate solution (27% SiO_2, 14% NaOH), *n*-heptane, chlorotrimethylsilane, *N*,*N*-dimethylacetamide, dodecane, styrene, *n*-butyl acrylate, triethylamine, 4-bromoacetophenone, chlorobenzene, bromobenzene, 1-bromo-4-nitrobenzene, niobium ethoxide, palladium (10 wt %) on alumina, palladium (10 wt %) on activated carbon, silica gel (70−230 mesh, BET surface area ~500 m^2/g) (Aldrich); hexadecyltrimethylammonium bromide (Alfa Chemicals); and allylpalladium chloride dimer (Strem Chemicals) were used as received.

Instrumentation. The powder X-ray diffraction (XRD) data were recorded on a Siemens D5000 $\theta-\theta$ diffractometer with nickel-filtered Cu Kα radiation. Transmission electron micrographs were taken on a JEOL 200CX transmission electron microscope equipped with a lanthanum hexaboride (LaB_6) gun operating at an accelerating voltage of 200 kV and with an objective aperture of 60 mm. Samples for transmission electron microscopy (TEM) were ground, sonicated in 2-propanol, and supported on a carbon-coated copper grid. Nitrogen adsorption isotherms were collected at 77 K on a Micromeritics ASAP 2010 Gas Sorption and Porosimetry System. Samples were typically prepared for measurement by degassing at 150 °C under vacuum until a final pressure of 10^{-2} Torr was reached. BET (Brunauer−Emmett−Teller) surface areas were determined over a relative pressure range of 0.005 to 0.20. Mesopore size distributions were calculated with the BJH (Brunauer−Joyner−Halenda) method off the adsorption branch of the isotherms. Diffuse reflectance infrared Fourier transform (DRIFT) spectra were collected with a Harrick HVC-DRA2 cell on a Bio-Rad FTS-60A spectrometer. ^{13}C and ^{29}Si solid-state magic angle spinning nuclear magnetic resonance (MAS NMR) spectra were obtained by Spectral Data Services, Inc. on a SDS270 instrument operating at a frequency of 270.618 MHz with an Oxford standard bore (54 mm) magnet and a home-built Nicolet-based spectrometer system with Henry Radio amplifiers for final RF generation.

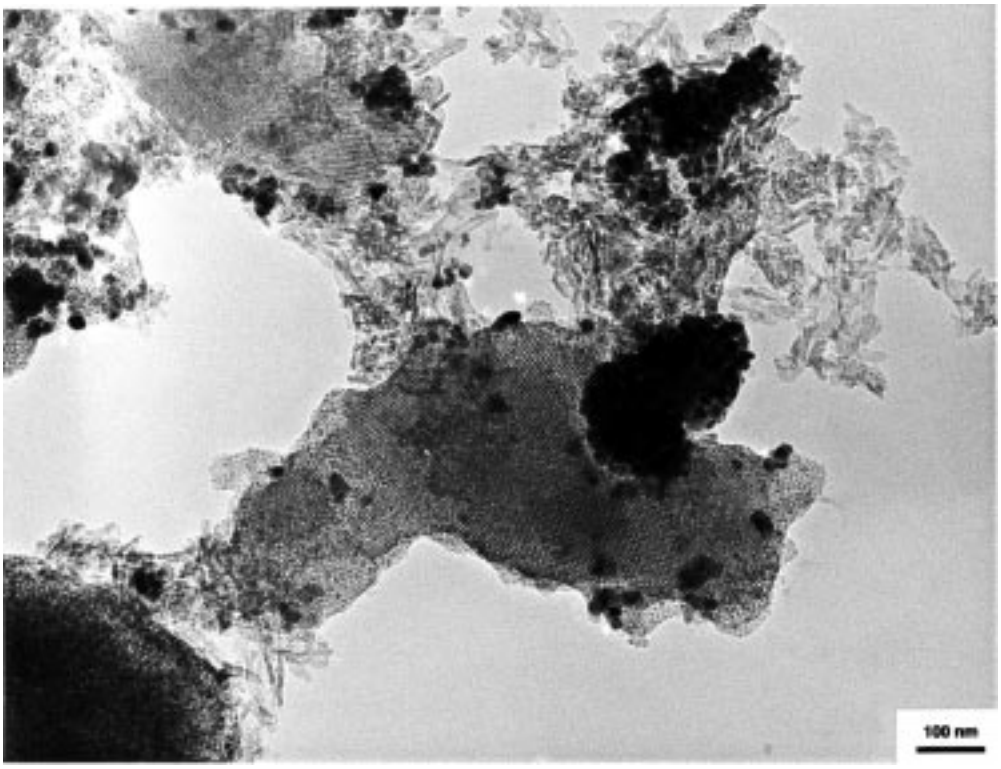

Figure 8. Transmission electron micrograph of the Pd-TMS11 catalyst recovered after a total TON of 3000 from the reaction between 1-bromo-4-nitrobenzene and *n*-butyl acrylate at 120 °C.

Modified Synthesis of Nb-MCM-41. Hexadecyltrimethylammonium bromide (15.9 g, 44.9 mmol) was dissolved in H_2O (1.2 L) and treated with sodium silicate (27% SiO_2, 14% NaOH) (100 g, 44.9 mmol) in distilled H_2O (0.4 L) and niobium ethoxide (1.27 g, 4 mmol) to give a white precipitate. After the mixture was stirred for 30 min, the pH value was adjusted to 11.5 with sulfuric acid (30%). The gel was aged at room temperature for 5 days before it was heated in pressure tubes to 80 °C for 7 days. The supernatant of the aged gel was decanted off and the resulting white residue was washed with H_2O (1 L) and EtOH (1 L). The isolated solid was dried in air at room temperature for 24 h before the material was calcined at 560 °C (ramp = 1 °C/min) for 6 h, giving mesoporous Nb-MCM-41 material (XRD: (100) 39.9 Å, (110) 22.5 Å, (200) 19.6 Å, (210) 14.8 Å; BET surface area = 997 m^2/g; BJH average adsorption pore size = 27.4 Å; elemental analysis (wt %): C < 0.1, H < 0.1, N < 0.01, Nb = 1.5). The introduction of niobium dopant increased the long-range pore-packing order of the mesostructure and led to thicker pore walls (18 Å) in comparison to undoped MCM-41 material (12 Å).

Silylation of Nb-MCM-41. Nb-MCM-41 (1.8 g) (XRD: (100) 38.4 Å, (110) 22.1 Å, (200) 19.2 Å, (210) 14.6 Å; BET surface area = 1004 m^2/g; BJH average adsorption pore size = 23.9 Å) was degassed at 150 °C under reduced pressure (10^{-2} Torr) for 6 h before being treated with chlorotrimethylsilane (8.56 g, 79 mmol) in *n*-heptane (100 mL). After the mixture was refluxed for 5 h, the supernatant was filtered off and the resulting solid was washed with pentane (3 × 100 mL). To ensure that the silanized support material was free of all solvent and silane residues, the material was dried under reduced pressure (10^{-2} Torr) at room temperature for 12 h, giving a white powder (XRD: (100) 38.4 Å, (110) 22.1 Å, (200) 19.2 Å, (210) 14.6 Å; BET surface area = 824 m^2/g; BJH average adsorption pore size = 21.4 Å; DRIFT: ν(C−H) 2966 (s), 2910 cm^{-1} (m); ^{13}C−CP/MAS NMR: δ −1.1 ppm [−Si(*C*H_3)$_3$]; ^{29}Si−CP/MAS NMR: δ −111.0 [*Si*−O−*Si*], −106.9 [*Si*−O−*Si*], 14.4 ppm [−*Si*(CH_3)$_3$]; elemental analysis (wt %): C = 6.4, H = 1.3, N < 0.05).

Palladium-Grafted Mesoporous Material (Pd-TMS11). (a) Nb-MCM-41 (0.5 g) (XRD: (100) 39.9 Å, (110) 22.5 Å, (200) 19.6 Å, (210) 14.8 Å; BET surface area = 997 m^2/g; BJH average adsorption pore size = 27.4 Å) was degassed at 600 °C under reduced pressure (10^{-2} Torr) for 6 h. The resulting material was loaded into a short-path frit and contained with glass wool under an inert atmosphere. A small round-bottom flask was filled with the red complex [Pd(η-C_5H_5)(η^3-C_3H_5)] (0.25 g, 1.2 mmol) and connected to the loaded frit that was further attached to a condensation bridge with an empty round-bottom flask. The apparatus (Figure 2) was evacuated, and a constant pressure (10^{-2} Torr) was maintained by cooling the empty round-bottom flask to −196 °C. The small round-bottom flask containing volatile palladium complex and the loaded frit were heated to 85 °C (ramp = 1 °C/min) with an oil bath. It is important that the level of the oil bath fully covers the bed of the porous material to ensure uniform grafting. During the heating process, the white Nb-MCM-41 material turned black and the excess volatile organometallic complex was condensed into the cooled round-bottom flask. The resulting solid was reduced under a stream of hydrogen (50 mL/min) at 350 °C for 3 h, giving a black powder designated Pd-TMS11 (XRD: (100) 39.6 Å, (110) 22.5 Å, (200) 19.6 Å, (210) 14.8 Å; BET surface area = 750 m^2/g; BJH average adsorption pore size = 26.1 Å; CO chemisorption: Pd dispersion = 32%, Pd surface area = 140 m^2/g (Pd metal); elemental analysis (wt %): Pd = 22.3).

(b) To reduce the loading of palladium on the mesoporous support, silanized Nb-MCM-41 material (XRD: (100) 38.4 Å, (110) 22.1 Å, (200) 19.2 Å, (210) 14.6 Å; BET surface area = 824 m^2/g; BJH average adsorption pore size = 21.4 Å) was used for the vapor grafting process. The silanized Nb-MCM-41 material (0.3 g) was treated with [Pd(η-C_5H_5)(η^3-C_3H_5)] (0.05 g, 0.23 mmol) following the vapor grafting preparation described under (a), giving a palladium-grafted Pd-TMS11^s catalyst with a significantly reduced metal content. The XRD pattern showed a (100) peak at 38.4 Å and distinct (110) and (200) peaks; the BET method gave 633 m^2/g of surface area with a BJH average adsorption pore size of 21.2 Å. CO chemisorption indicated a Pd dispersion of 25% and a Pd surface area of 110 m^2/g (Pd metal). Elemental analysis gave 1.6% Pd by weight.

(c) To scale up the preparation of Pd-TMS11^s, a fluidized bed reactor was built that enabled multigram-scale synthesis of the catalyst. In a typical preparation, silanized Nb-MCM-41 (15 g) and volatile organometallic precursor [Pd(η-C_5H_5)(η^3-C_3H_5)] (0.5 g, 2.3 mmol) were loaded into the fluidized bed reactor, separated by a porous frit, under an inert atmosphere. After the sealed reactor was exposed to air, a stream of argon was vented through the reactor, generating the fluidized bed. The column setup was warmed (ramp = 1 °C/min) to 125 °C for 2 h with heating tapes. The excess volatile palladium complex was recycled from the top of the reactor column, while the palladium-grafted Nb-MCM-41 material was isolated as a grayish-black powder from the fluidized bed section of the column. In the final step of the preparation, the material was reduced under a stream of hydrogen at 350 °C for 3 h, giving Pd-TMS11^s.

Palladium Deposition onto Nb-MCM-41 *via* Impregnation. (a) A suspension of Nb-MCM-41 (1.0 g) (XRD: (100) 43.8 Å, (110) 24.5 Å, (200) 21.2 Å, (210) 16.0 Å; BET surface area = 823 m^2/g; BJH average adsorption pore size = 21.4 Å) in hexane (200 mL) was treated with a solution of [Pd(η-C_5H_5)(η^3-C_3H_5)] (0.05 g, 0.23 mmol) in hexane (50 mL). The reddish-brown slurry was stirred for 6 h at room temperature. The suspension was filtered and the solid residue was washed with hexane (3 × 50 mL). After the impregnated solid was dried under reduced pressure, the material was reduced under a stream of hydrogen at 350 °C for 3 h, giving a gray powder (XRD: (100) 41.4 Å, (110) 23.0 Å, (200) 20.0 Å, (210) 14.9 Å; BET surface area = 710 m^2/g; BJH average adsorption pore size = 20.4 Å). Carbon monoxide chemisorption analysis indicated a metal dispersion of 17% and a metallic surface area of 78 m^2/g (Pd metal). Elemental analysis gave 4.4% Pd by weight.

(b) A suspension of Nb-MCM-41 (1.0 g) (XRD: (100) 41.0 Å, (110) 23.1 Å, (200) 20.0 Å, (210) 15.0 Å; BET surface area = 1041 m^2/g; BJH average adsorption pore size = 24.3 Å) in distilled H_2O (200 mL) was treated with a solution of $PdCl_2$ (100 mg, 0.56 mmol) in distilled H_2O (50 mL). The reddish-brown slurry was stirred for 6 h at room temperature. The suspension was filtered and the solid residue was washed with distilled H_2O (3 × 250 mL). After the impregnated solid was dried at 150 °C for 12 h, the material was reduced under a stream of hydrogen at 350 °C for 3 h, giving a black powder (XRD: (100) 40.4 Å, (110) 22.8 Å, (200) 19.8 Å, (210) 14.9 Å; BET surface area = 948 m^2/g; BJH average adsorption pore size = 24.0 Å). Carbon monoxide chemisorption analysis indicated a metal dispersion of 9% and a metallic surface area of 40 m^2/g (Pd metal). Elemental analysis (wt %) gave C = 0.2, H = 0.6, N < 0.05, Cl = 0.2 and Pd = 1.0.

Palladium Deposition onto Silica Gel *via* Impregnation. A suspension of silica gel (1.0 g) in distilled H_2O (200 mL) was treated with a solution of $PdCl_2$ (100 mg, 0.56 mmol) in distilled H_2O (50 mL). The reddish-brown slurry was stirred for 6 h at room temperature. The suspension was filtered and the solid residue was washed with distilled H_2O (3 × 250 mL). After the impregnated solid was dried at 150 °C for 12 h, the material was reduced under a stream of hydrogen at 350 °C for 3 h, giving a black powder (BET surface area = 437 m^2/g; carbon monoxide chemisorption analysis showed a metal dispersion of 4% and a metallic surface area of 18 m^2/g (Pd metal); elemental analysis (wt %): C < 0.1, H = 0.5, N < 0.05, Cl = 0.3, Pd = 2.0).

General Procedure for Heck Olefination of Aryl Halides. A 250 mL three-necked flask equipped with a thermometer and a reflux condenser was charged with aryl halide (49 mmol), styrene (6.9 mL, 60 mmol) or butyl acrylate (8.6 mL, 60 mmol), triethylamine (7.3 mL, 52.4 mmol), dodecane (7.2 mL, 31.7 mmol), and *N*,*N*-dimethylacetamide (48 mL). The palladium catalyst (Pd-TMS11) was added through a funnel and the reaction mixture was heated to 120 or 170 °C (mol % of the catalyst used, reaction time, and temperature are shown in Table 2). To monitor the reaction, 0.2 mL samples were taken in regular intervals, diluted with *N*,*N*-dimethylacetamide, filtered over a bed of Celite, and analyzed by gas chromatography and mass spectrometry. After completion of the reaction, the mixtures were quenched with H_2O (400 mL) and the organic products extracted with diethyl ether (3 × 200 mL). The combined organic phases were dried over $MgSO_4$, filtered, and concentrated under reduced pressure. Separation of the *e*/*z*-isomers was carried out by chromatography with silica gel with pentane/diethyl ether (1:1) solvent mixtures. Recrystallization of the

resulting material from concentrated diethyl ether solutions at −10 °C gave analytically pure product. The catalyst was filtered from the aqueous phase. The solid was washed with ethanol (2 × 200 mL) and diethyl ether (2 × 200 mL) and dried at 150 °C for several hours to give a black solid.

Heterogeneity Test. To ensure that the catalysis runs were based on a heterogeneous pathway, two test experiments were undertaken: (a) The reaction was carried out in a similar manner as the general procedure for Heck reactions, with the exception that the catalyst was filtered off via cannular after approximately 20% conversion. The resulting solution was heated under the identical reaction condition for an additional 2 h and analyzed for further conversion. No further reaction was noted after the catalyst removal. (b) The reaction was carried out in a similar manner as the general procedure for Heck reactions, with the exception that a drop of elemental mercury was added to the reaction mixture after 20% conversion. The reaction stopped upon mercury introduction, and no further conversion was noted. Both experiments indicated that the Heck reactions we investigated followed a heterogeneous pathway.

Acknowledgment. We thank Dr. T. J. Garrett-Reed and M. Frongillo (M.I.T. CMSE) for their assistance with transmission electron microscopy. Financial support from the National Science Foundation (CTS-9257223), David and Lucile Packard Foundation, and M.I.T. UROP Office (D.W.W.) is gratefully acknowledged.

JA971637U